Dynamics and Laser Processing of Functional Fluoride Organic Surfaces at VUV Wavelengths

Evangelia Sarantopoulou[*], Zoe Kollia*, Margarita Chatzichristidi**, Antonios Douvas**, Panagiotis Argitis**, Spomenka Kobe*** , Alkiviadis-Constantinos Cefalas*.
[*]*National Hellenic Research Foundation, TPCI,48 Vas. Constantinou Aven. Athens 11635 Greece*
email: ccefalas@eie.gr
[**]*Institute of Microelectronics, NCSR Demokritos, 15310 Agia Paraskevi, Greece*
[***]*Jožef Stefan Institute,Department of Nanostructured Materials, Jamova 39, SI-1000 Ljubljana, Slovenia*

The 157 nm laser ablation efficiency and the resolution limit of micro-patterned structures of fluoride based organic surfaces (polymers, monomers) depend on both the material's properties and the irradiation conditions, such as the laser's fluence and the beam diameter. For 1-10 mJ/cm^2 and beam diameter less than 10 μm, accumulation of dissociated products on the irradiated surfaces prevented efficient laser ablation . The surface's etching rate for beam diameter larger than 10 μm, was linearly depended on the fluence and it had the capacity of sub-nanometer resolution in the direction of the laser beam (perpendicular to the irradiated surface). In addition, it was found that the etching rate was proportional to the photodissociation rate of the materials (out-gassing rate).
DOI: 10.2961/jlmn.2008.01.0006
Keywords: VUV polymer etching, surface treatment, polymer out gassing, micro fabrication, micromachining, light induced nanostructures, fluoropolymers.

1. Introduction

The physical principles of fabricating microstructures on thin films with laser light in the Vacuum Ultraviolet (VUV) region of the spectrum (100-180 nm), on fluoride organic films are presented in this communication. The applications span a wide range in science and engineering. A number of novel approaches and methodologies were developed recently, suitable for micro-fabrication of devices containing biological systems. New materials were designed and efficient patterning methods were proposed for modern multi-analytic devices [1]. Among the variety of patterning techniques [2, 3], laser ablation is an efficient direct-writing method, which was proposed for bio patterning [4]. It has certain advantages, as it does not require masks and does not include wet steps that might denature proteins or complicate the processes. The methodology is targeting the specification of surface functionality and increasing the writing density with parallel improving of detection efficiency for sensing applications. The 157 nm F_2 laser is able to modify the chemical functionality of surfaces during patterning and to improve resolution. Major applications include surface preparation of biological films, preservation of cultural heritage artifacts, biology and fabrication of bio-arrays [5, 6]. The common denominator of these applications is based on the fact that nano-fabrication at VUV wavelengths allows atomic resolution depth control, induces chemical changes and at the same time enhances surface functionalization, with the most prominent application that of DNA micro-array fabrication. [7-15]. On the other hand, fluoride organic films are good candidates for such applications. The technology was applied using Poly (2,2,2-trifluoromethyl methacrylate), PTFEMA, for bio-array micro-fabrication [6] with the following advantages: 1) It allows surface preparation at VUV wavelengths with localized chemical changes and controlled surface roughness [16-20]. 2) It stimulates surface functionality.. 3) It enhances detection sensitivity and accelerates hybridization time by optimizing the patterning structures and specifying the limits to control the surface etching rate on the molecular level. In this communication we report on the ablation efficiency and the surface morphology of 157 nm laser micro-patterned fluoride based organic surfaces. They both depend on material's properties and the irradiation conditions. The resolution limit of micro- patterned structures depends on both the laser's fluence and beam's diameter. Accumulation of dissociated products on the surfaces prevents efficient laser ablation with beam diameter less than 10 μm at 1-10 mJ/cm^2. The etching rate at larger beam diameters was a linear function of the fluence and it was controlled with nanometer resolution in the direction perpendicular to the surface. In addition, it was found that it was proportional to the photodissociation rate of materials (out-gassing rate). The outgassing rate of four different phenyl- prop based fluoride monomers was comparable to the rate of PTFEMA and Teflon polymers and with similar photochemical response and surface etching rate. The overall assessment of the method suggests that, for these materials, fabrication of arrays was possible for beam diameter >10μm. The surface morphology and the thickness loss was controlled by adjusting the laser's parameters. By applying this methodology, the resolution of the film's etching rate was ~ 0.5 nm in the Z direction per pulse at ~ 1mJ/cm^2. Generally it depends on the materials and the preparation conditions of the film.

2. Experimental

Micro array patterning on PTFEMA polymer substrates was demonstrated and the best results were achieved with laser beam diameter > 10μm at 1mJ. Patterning with resolution better than 10 μm was difficult to be achieved on the PTFEMA and the fenyl–prop monomers, due to the accumulation of material on the illuminated areas and

swelling of the substrate from volume ablation. Patterning with beam diameter > 20 μm at ~ 1 mJ, provides pillar-free surfaces. The materials were placed on a X-Y-Z-Θ computer controlled translation stage and the laser beam was focused with a CaF_2 projection optics.

Fig. 1 157 nm micro-machining stage. The computer controlled CCD camera, the X-Y-Z-Θ micro- translator, the focusing optics and the sample holder are indicated.

Different types of micro etched surfaces and shapes were obtained on films, spin/dip coated on Si substrates. With this experimental configuration, the resolution of the focused beam on the target was adjustable from 3 mm to 10

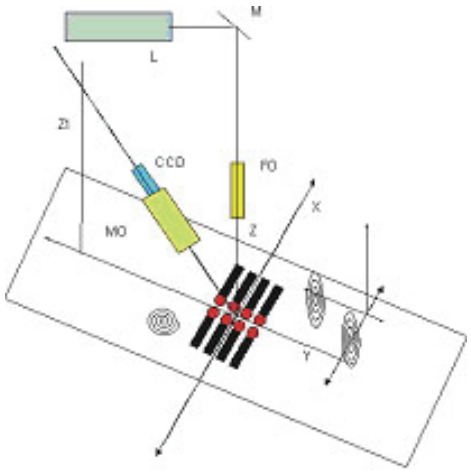

Fig. 2 Schematic lay out of the micro-machining stage with CCD imaging system for automatic alignment and pre-set exposure conditions, operating in real-time feed back mode. L: 157 nm laser, M: VUV mirrors, FO: Focusing optic, CCD: CCD camera and optical imaging system of the processed area.

μm. An improved version of the system allowed further flexibility, accuracy and automatic alignment by interfacing it to a CCD imaging system operating in a real-time feed back mode, Fig. 1, 2. The system has 2 μm translation and position resolution during the successive steps of the manufacturing processes.

In each step, the organic films, were taken out from the micromachining stage, then they were processed and finally were placed back to proceed with the next step, and so on. The micro-arrays of Fig. 3 were fabricated using a three-lens projection system. With the additional use of two mirrors, improved shaped circular spots on the polymer were obtained, Fig. 4. For laser's beam spot-size less than ~ 15 μm, the ablation efficiency was reduced progressively.

Furthermore, photochemical changes on the molecular level can be evaluated by applying mass-spectrometry and atomic force microscopy (AFM) imaging of the irradiated surfaces. With the application of these methodologies the thickness loss of four different fluorine monomers was measured using a similar methodology as for the PTFEMA polymer [6]. The monomers were the following (S1): (2E)-1,3 diphenylprop-2-en-1-one, (S2): (2E)- 3 (pentafluorophenil)-1-1-phenylprop-2-en-1-o, (S3): (2E)- 1-1(pentafluorophenil)-3-phenylprop-2-en-1-o and (S4): (2E)- 1-3 bis(pentafluorophenil)- prop-2-en-1-one. The fluoro-monomers were dissolved in CH_2Cl_2 and then, the films were grown by slow evaporation of solutions on Si wafers.

Results and discussion

I. VUV Photo-dissociation

Excitation of organic materials with VUV light is followed by dissociation. Part of the energy of the absorbed photon is expended in breaking the chemical bonds, and forming molecules with smaller number of atoms. A fraction of photon energy is converted to translational energy of the photo-fragments and eventually the electronically excited molecules relax to the ground electronic state(s) either radiatively or non-radiatively.

At VUV wavelengths, excitation from the ground electronic state W_1 to the excited electronic state W_2 is followed by dissociation. The energy transfer is considerably faster than vibration relaxation. The dissociation probability Γ, is given by the photo-dissociation rate Γ,

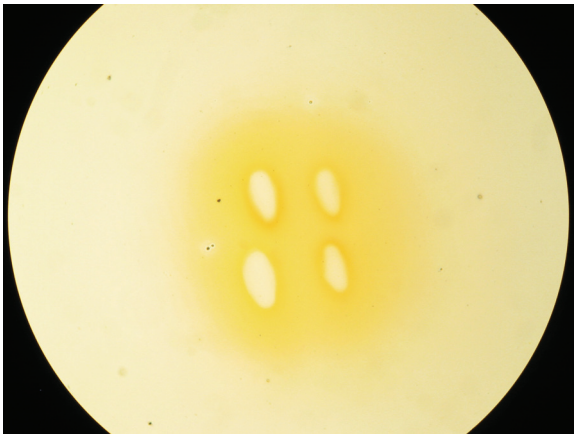

Fig. 3 Micro-array patterning on PTFEMA substrates. The size of each one of the oval spots is 10 X 20 μm.

which in most cases is the rate of organic film's etching [6]. The photo-dissociation rate is given by the equation:

$$\Gamma = \frac{4\pi V^2}{\upsilon\hbar|S_1 - S_2|} \quad (1)$$

It relates the dissociation rate with the molecular parameters $S_{1,2}$, $V(R)$, and υ and it is inversely proportional to the difference of the slops $S_{1,2}$ of the two potential surfaces at the point of intersection. V is the dipole moment of the

optical transition and υ is the mechanical action of the molecular system. Taking into consideration that the photo-dissociation rate at low laser energy is independent from the beam's parameters, eqn.1, the photo-dissociation rate at VUV wavelengths is an intrinsic molecular property. In other words, the etching rate of polymers
at VUV wavelengths is taking place even with the lowest number of photons possibly available. We expect therefore one photon to break one molecular bond of the parent organic molecule (e.g polymers, monomers, etc) and subsequently to release at least one photo-fragment. The above theoretical considerations were previously confirmed experimentally for a large number of different organic molecules [6]. The photo-dissociation and the etching rate of various organic materials were measured by applying different experimental methodologies such as dynamic out-gassing, AFM imaging and VUV absorption spectroscopy [6].

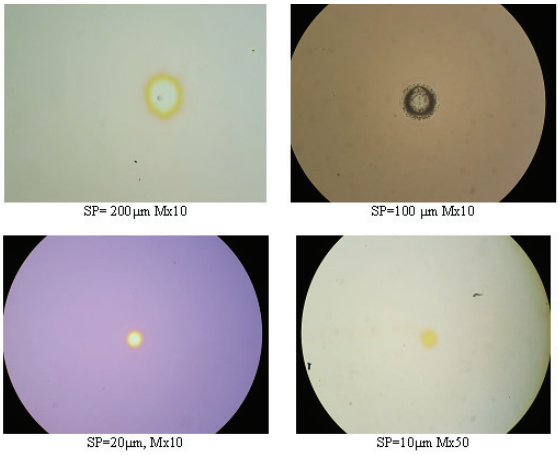

Fig. 4 Circular beam profiles on PTFEMA. The spatial resolution of the etched areas from top to bottom is 200, 100, 20, 10µm.

II. Out gassing rate of fluoro-polymers/monomers.

The photo-dissociation rate of polymers at a given wavelength is an indication of the level of surface and volume modifications and the chemical changes induced by light. The molecular photo-dissociation at low energy (< 1mJ) is localized mainly on the surface of the films and giving structures with perfectly sharp edges. The process is therefore important in micro/nano engineering processing of materials. The sharpness of the step across the boundary between the irradiated/non-irradiated areas depends on the material as well, Fig.5.

One of the experimental methodologies of determining the photo-dissociation rate at 157 nm, is to monitor the background pressure inside the stainless-steel (SS) vacuum chamber where the organic films were placed following their irradiation at 157 nm (dynamic out-gassing). Generally, the out-gassing rate is the amount of moieties released in the gas phase per unit time and surface area from the organic film and it is expressed in mbar in a volume of a litter per sec per square centimeter (mbar l s^{-1} cm^2). Prior to irradiation, out-gassing of SS vacuum chamber was measured under different experimental conditions (static out-gassing). It was found that contamination of the SS chamber was taking place following irradiation
of materials at 157 nm. Thus the number of photo-

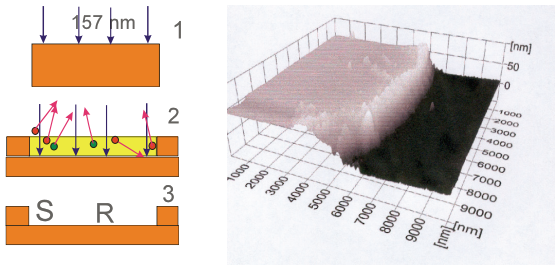

Fig. 5 Left: Schematic lay out of VUV ablation process. From top to bottom: 1) VUV light falling on the surface of organic films. 2) The photons are penetrating within the volume of the film (yellow area). 3) The yellow area is ablated through photo-dissociation giving sharp edges at the boundaries between irradiated/non-irradiated area. Right: AFM image of the edge between exposed / non-exposed areas at 157 nm (~ 1 nJ/cm^2).

fragments ejected out from the surface or the volume of the polymer can be evaluated. On the other hand, from the energy of the laser beam, the number of ejected photo-fragments from the surface of the polymer film per photon can be estimated. The out-gassing rate of fluorine monomers (S1-4) is indicated in Fig. 6. Taking into consideration that the increase of the background pressure inside the SS chamber was $\delta P \sim 10^{-5}$ mbar at 1mJ, the number of out-gassed atoms and molecules, ejected out from the surface of the illuminated areas

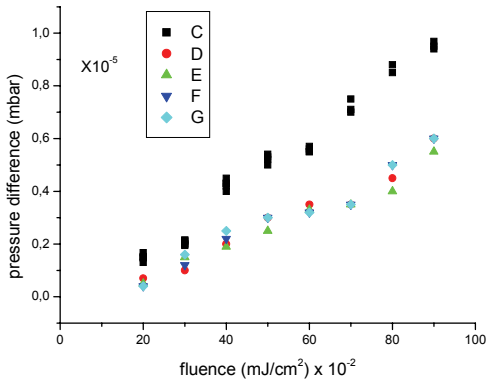

Fig. 6 Pressure gradient from out-gassing of S1-4 at different fluence. (D–S1, E-S2, F-S3, G-S4). For comparison the out-gassing rate of a Si based copolymer [21] is indicated, C.

was ~ $\delta n = 1.54 \times 10^{15}$ on the average. As 1mJ carries 7.9×10^{14} photons, 1 photon ejects on the average several atomic/molecular species. The indicative out-gassing rates (pressure differences) of the S1-4 fluoride monomers at different fluence are tabulated in table 1.

Fluence (mJ/cm^2)	δP(mbar)x10^{-5}
20	0.1
40	0.27
70	0.42
100	0.76

Table 1 Average out-gassing rates (pressure differences) of the S1-4 fluoride monomers.

The composition of the out-gassed moieties was analyzed with mass spectroscopy. The mass spectrum of S2 is indicated in Fig. 7. Despite the fact that the background pressure in the detection area could be as low as 10^{-8} mbar, the pressure within the high vacuum chamber with the S2 polymer inside was ~ 9×10^{-7} mbar. Photofragments with m/e less than 40 were mainly detected, a fact, which indicates that the S2 monomer is photodissociated at small photo-fragments far more efficient at 157 nm in agreement with previous results, [22, 23]. The peaks at 19, 31, 43, 50, 69, 81, 100 amu correspond to the F, CF, C_2F CF_2, CF_3, C_2F_3 and C_2F_4 moieties respectively. The low abundance at higher m/e was due to further dissociation from 157 nm photons. On the contrary, at longer wavelengths and for Teflon, parts of material were removed without degradation or decomposition and higher values of m/e were recorded in the mass spectra, [24, 25].

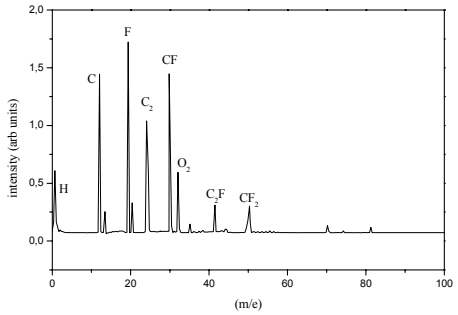

Fig. 7 Mass spectrum of S2. The background pressure was 9×10^{-7} mbar.

III. AFM imaging

With the application of AFM imaging technique, the relation between thickness loss and laser energy was established by measuring the thickness loss (step) of the boundary between illuminated / non-illuminated areas. This method does not require ultra high vacuum, contrary to dynamic out-gassing . At the same time, the surface morphology of the exposed/non-exposed areas is revealed. In Fig. 8a, b the edge of the PTFEMA polymer is clearly seen, and from Fig.8b it was measured to be 0.7 nm for 1 mJ/cm^2, in agreement with previous results [6] and the theoretical predictions of eqn 1.The etching rate was linearly depended on the fluence. Similarly the etching rate for the S1-4 monomers was 0.5, 0.6, 0.8, 1 nm respectively, for 1 mJ/cm^2 and it was linearly depended on laser's fluence between 1-10 mJ/cm^2. The fluence was controlled with the energy of the beam by keeping constant the diameter of the beam.

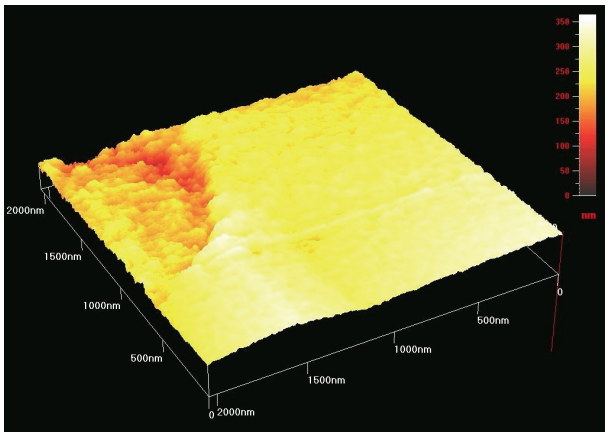

Fig. 8a AFM image of PTFEMA following laser irradiation at 157 nm. The edge between irradiated/non-irradiated areas can be clearly seen.

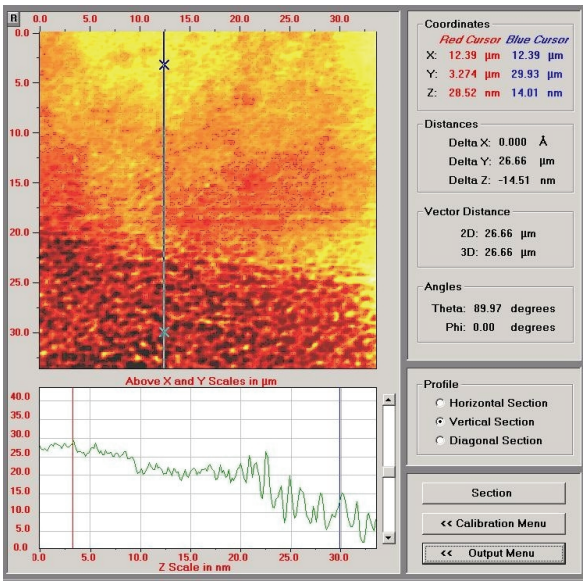

Fig. 8b 2D AFM image of irradiated/non-irradiated areas. The step of the edge is 14.01 nm.

Besides the application of the above methodologies to determine the etching rate of organic films, an additional method was applying previously. A thin polymeric film of known thickness was deposited on a CaF_2 substrate by spinning and the absorption coefficient of the film was measured with VUV absorption spectroscopy. Following the experimental procedure, part of the film was etched at 157 nm at a given laser fluence. The absorbance of the etched film was measured again, [6] and the experimental data were fitted to the Beer's low. The thickness loss of the etched film was thus evaluated, and a direct relationship between the film thickness loss and the laser energy at 157 nm was established, verifying thus a linear rela-

tionship between them, as it is expected from eqn. 1, [6].

IV. Surface morphology

At higher laser energy, explosive dissociation within the sample's volume rapidly increases the pressure. For given laser energy, reduction of the size of the beam diameter, confines the same amount of photons, (and thus dissociative moieties), within a smaller volume space in the sample, increasing thus the collision rate and the pressure within the irradiated volume. In the case of higher pressure, the material will be removed through surface ablation accompanied by surface swelling.

Furthermore, the initial surface morphology, the density and the presence of the size defects on the polymer surface, are important during the interaction of radiation with matter at 157 nm as a fraction of the photons was transmitted within the polymer volume under the surface.

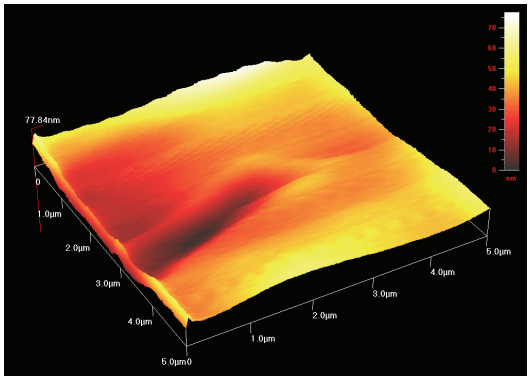

Fig. 9 AFM image of a surface dip of the irradiated area due to volume ablation. At lower laser fluence, the pressure gradient was not high enough to support the surface's swelling. The photo-fragments were removed mainly from the volume inside the film and eventually the irradiated area collapsed in a 3 μm x 3 μm x 40 nm dip. The area was illuminated with 100 laser pulses (15 μm laser beam, 1mJ/cm^2 per pulse).

The penetration depth (absorption coefficient), depends on the amount of the surface and the volume defects with size 1-5 nm, which further increase the penetration depth. In this case, the volume dissociation is predominant over surface dissociation and the polymer's surface is accompanied by swelling. In the case of lower energy, the dissociated products, escape from the polymer's volume and the illuminated area shrinks with the appearance of a surface dipping, Fig.9.

Swelling and dipping is the dominant process at smaller beam diameters, where the dissociation rate from inside the polymer's volume is higher than from surface. For PTFEMA, either non-ablative swelling or dipping was the predominant process, when the surface was irradiated with 100 laser pulses and with a 10 μm beam diameter at 1 mJ/cm^2. The surface was swelling by ~ 50 nm and around the edges, the surface dipping can be clearly seen. Volume ablation was not observed for Teflon samples [6]. Besides volume ablation, in the case of a laser spot of ~10 μm, enhanced collision rate of the ejected photofragments within the plume above the surface, recombination of dissociated photoproducts and fast relaxation were taking place. The photoproducts in this case, were not efficiently removed from the surface, but they agglomerate in the form of pillars, Fig. 10. The formation of the negative charged F^-, CF^{-1} photo fragments in the ablative plume, enhances the collision rate further in comparison to different types of organic films. The formation of nano-pillars with dimensions ranging from 10 nm to 1 μm was observed for both PTFEMA and Teflon [6]. Surface ablation of PTFEMA was observed previously and on the average 0.5 nm thin layers of polymer were removed at 1mJ/cm^2 [6]. In the case of laser spot size larger than

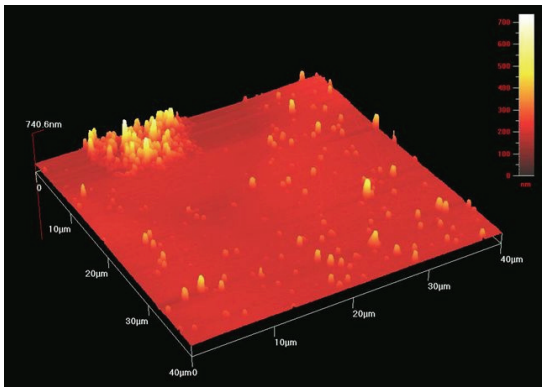

Fig. 10 Stacking of dissociated products on the surface of the polymer. When the laser spot size was < 10μm, the dissociated products were stuck on the polymer surface forming pillars due to the enhanced collision rate. The columns had different size (nm/μm). The area was illuminated at 1 1mJ/cm^2.

20 μm, ablation was taking place predominantly from the surface of the polymer. As it has been experimentally demonstrated, efficient laser ablation of the polymers is taking place when the spot size of the laser beam was focused to dimension higher than 10 μm. For beam diameter smaller than ~ 10 μm, the material was difficult to be removed by ablation in a reasonable time-scale and with good surface quality. At higher laser fluence, the overall assessment of the methodology indicates that, fabrication of micro-arrays in PTFEMA and the fluoromonomers S1-4 was fast and efficient for laser beam diameters > 20μm. Ablation rate of polymer surfaces under vacuum conditions was one order of magnitude higher than ablation in nitrogen. However contamination of the expensive projection optics by the out-gassed products prevents the long-term ablation under vacuum conditions.

Conclusions

The resolution limit of micro-patterned structures of fluoride based organic surfaces (polymers, monomers) and the etching rate depends on both the laser's fluence and beam's diameter. With beam diameters larger than 10 μm, the etching rate is a linear function of the fluence. In addition, the surface's etching rate was proportional to the photodissociation rate and with similar photochemical response at 157 nm for the fluoride materials. Light induced chemical changes have the advantage of multi functionality of surfaces for a variety of applications.

References

[1] R. Langer, and D. A. Tirell: Nature, 428, (2004) 487.
[2] M. Schena, D. Shalon, R. W. Davis, and P.O. Brown: Science, 270, (1995) 467.

[3]. S. P. A. Fodor, J. L. Read, M. C. Pirrung, L. T. Stryer, A. Lu, and D. Solas: Science 251, (1991) 767.
[4] Y. Martelé, K. Callewaert, K. Naessens, P. V. Daele, R. Baets, and E. Schacht: Mater. Sci. & Eng. C, 23, (2003) 341.
[5] A. C. Cefalas, E. Sarantopoulou, E. Gogolides, and P. Argitis: Microelectron. Eng. 53, (2000)123.
[6] E. Sarantopoulou, Z. Kollia , A. C. Cefalas , Z. Samardija, and S. Kobe: Thin Solid Films, 495, (2006) 45; A. C. Cefalas, E. Sarantopoulou, and Z. Kollia: Appl. Phys. A73, (2001) 571; E. Sarantopoulou, Z. Samardžija, S. Kobe, Z. Kollia, and A. C. Cefalas: Appl. Surf. Sci., 208-209, (2003) 311; Z. Kollia, E. Sarantopoulou, A. C. Cefalas, S. Kobe, and Z. Samardžija: Appl. Phys. A 79, (2004) 379; E. Sarantopoulou, Z. Kollia, A. C. Cefalas, S. Kobe and Z. Samardžija: Journ. Biolog. Physics 29, (2003)149; E. Sarantopoulou, Z. Kollia, and I. Gomoiu: Appl. Phys. A83, (2006) 663.
[7] A. M. Douvas, P. S. Petrou, S. E. Kakabakos, K. Misiakos, P. Argitis, E. Sarantopoulou, Z. Kollia, and A. C. Cefalas: Anal. Bioanal. Chem., 381, (2005) 1027.
[8] Z. Kollia, E. Sarantopoulou, A. C. Cefalas, and S. Kobe: Appl. Surf. Sci., 248, (2005) 248.
[9] D. D. Shoemaker, E. E. Schadt, C. D. Armour, Y. D., He, P. Garrett-Engele, P.D. McDonagh, and P. M. Loer: Nature, 409 (6822), (2001) 922.
[10] G. MacBeath and S. L. Schreiber: Science, 289(5485), (2000) 1760.
[11] T. A. Taton, C. A. Mirkin, and R. L Letsinger: Science, 289(5485), (2000) 1757.
[12] J. D. Cortese: The Scientist, 14 (11), (2000) 26.
[13] D. J. Lockhart and E.A Winzeler: Nature, 405(6788), (2000) 827.
[14] J. Fritz, M. K. Baller, H. P. Lang, H. Rothuizen, P. Vettiger, E. Meyer, H. Guntherodt, C. Gerber, and J. K. Gimzewski: Science, 288(5464), (2000) 316.
[15] J. D. Cortese: The Scientist 14, (2000) 25.
[16] M. Lapczyna, and M. Stuke: Appl. Phys., A66 (1998) 473.
[17] D. Bratton, Da Yang, J. Dai and C. K. Ober: Polym. Adv. Technol., 17, (2006) 94.
[18] V. Parihar, R. Singh, and R. Sharangpani, S. D. Russell, and C. A. Young: IEEE Trans. Elect. Dev.47, (2000) 1463.
[19] P. H. Holloway and G. E. McGuire, and R. Singh: ¨Handbook of Compound Semicondactor: Rapid Thermal Processing¨ (ed. Park Ridge, NJ Noyes 1995), chap 9, pp.442 (Books).
[20] T. Lippert: Plasma Processes and Polymers, 2, (2005) 525.
[21] E. Sarantopoulou, Z. Kollia, K. Kocevar, I. Musevic, S. Kobe, G. Drazic, E. Gogolides, P. Argitis and A. C. Cefalas: Mat. Sci. and Eng. C., 23, (2003) 995.
[22] S. G. Hansen, and T. E. Robitaille: Appl. Phys. Lett., 43, (1988) 717.
[23] M. Stuke, and Y. Zhang: Laser Processes for Microlectronic Applications (Eds: J.J. Ritsko, D.J. Ehrlich, M. Kashiwagi) The Electrochemical Society 1986) p70. (Conference Proceedings).
[24] L. J. Matienzo, J. A. Zimmerman and F. D. Egitto: J. Vac. Sci. Tech., A 12, (1994) 2662.
[25] G. Blanchet, and C. Fincher, Jr.: Adv. Matter., 6, (1994) 881.

(Received: April 24, 2007, Accepted: November 26, 2007)